Electronic Supplementary Material (ESI) for Materials Chemistry Frontiers.

Supplementary Information

Activating self-supported NiPd electrode by laser-direct-writing for efficient hydrogen evolution reaction

Zihan Zhou, Liyang Xiao, Jun Zhao, Miao Zhou, Jingtong Zhang, Xiwen Du, Jing Yang*

Institute of New-Energy Materials, Key Laboratory of Advanced Ceramics and Machining Technology of Ministry of Education, School of Materials Science and Engineering, Tianjin University, Tianjin 300072, China.

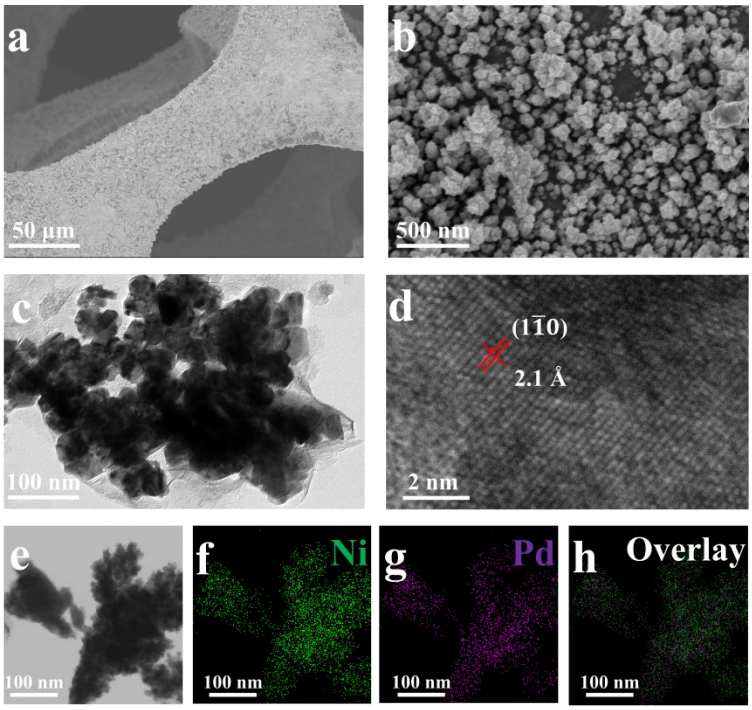

Supplementary Figure 1. a-b SEM images of the D-$Ni_{3.5}Pd$/NF electrode. **c** TEM image of the D-$Ni_{3.5}Pd$ nanaparticles removed from the D-$Ni_{3.5}Pd$/NF electrode by scraping off. **d** HR-TEM image of one D-$Ni_{3.5}Pd$ nanaparticle. **e** STEM image and **f-h** elemental mapping images of the D-$Ni_{3.5}Pd$ nanoparticles.

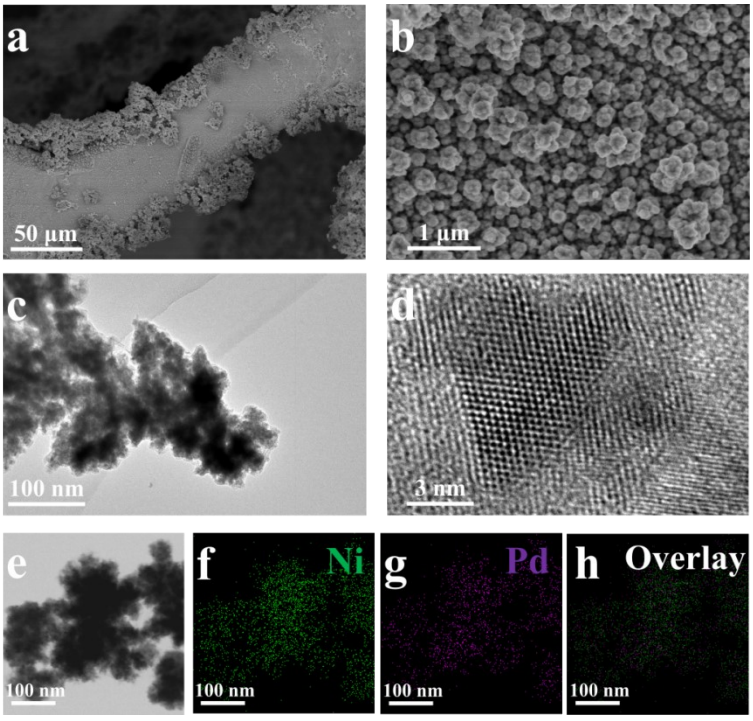

Supplementary Figure 2. a-b SEM images of the $Ni_{3.5}Pd$/NF electrode. **c** TEM image of the $Ni_{3.5}Pd$ nanaparticles removed from the $Ni_{3.5}Pd$/NF electrode by ultrasonication. **d** HR-TEM image of one $Ni_{3.5}Pd$ nanaparticle. **e** STEM image and **f-h** elemental mapping images of the $Ni_{3.5}Pd$ nanoparticles.

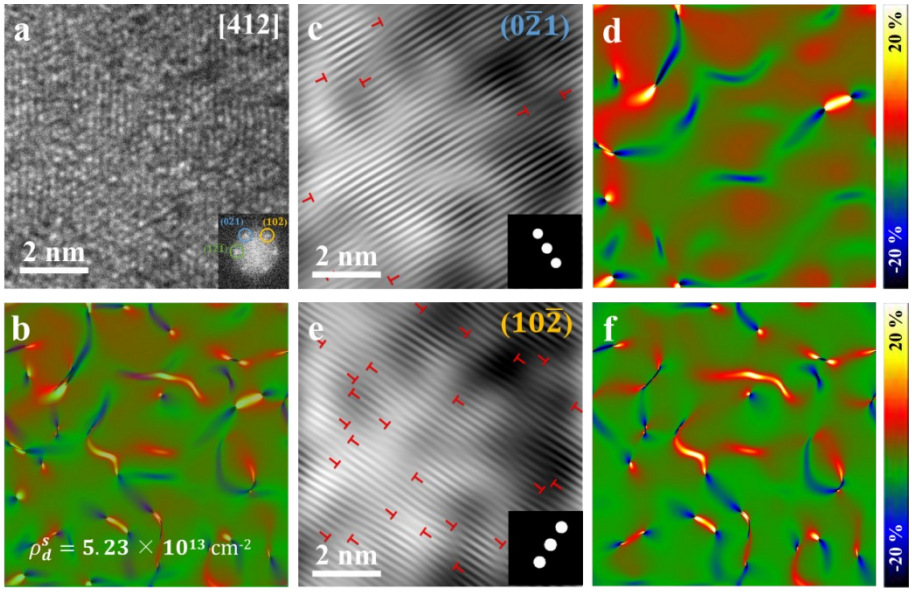

Supplementary Figure 3. a HR-TEM image of the D-$Ni_{3.5}Pd$ nanoparticles (removed from the D-$Ni_{3.5}Pd$/NF electrode by ultrasonication) along [412] zone axis and corresponding electron diffraction pattern by performing FFT on (**a)** ; **b** An overlay of strain components ε_{xx} and ε_{yy}, superimposed with the HR-TEM image, suggesting a high dislocation density of $\rho_d^s = 5.23\times10^{13}$ cm^{-2} on (412) plane. **c** IFFT image corresponding to diffraction spot $0\bar{2}1$, showing the $(0\bar{2}1)$ plane containing edge dislocations marked with symbol ⊥. **d** Contour plot of the strain component ε_{xx} by GPA analysis on (**c**). The color legend represents different strain, *i.e.*, green to dark blue relates to compressive strain and red to bright yellow corresponds to tensile strain. **e** IFFT image corresponding to diffraction spot $10\bar{2}$, showing the $(10\bar{2})$ plane containing edge dislocations marked with symbol ⊥. **h** Contour plot of the strain component ε_{yy} by GPA analysis on (**e**).

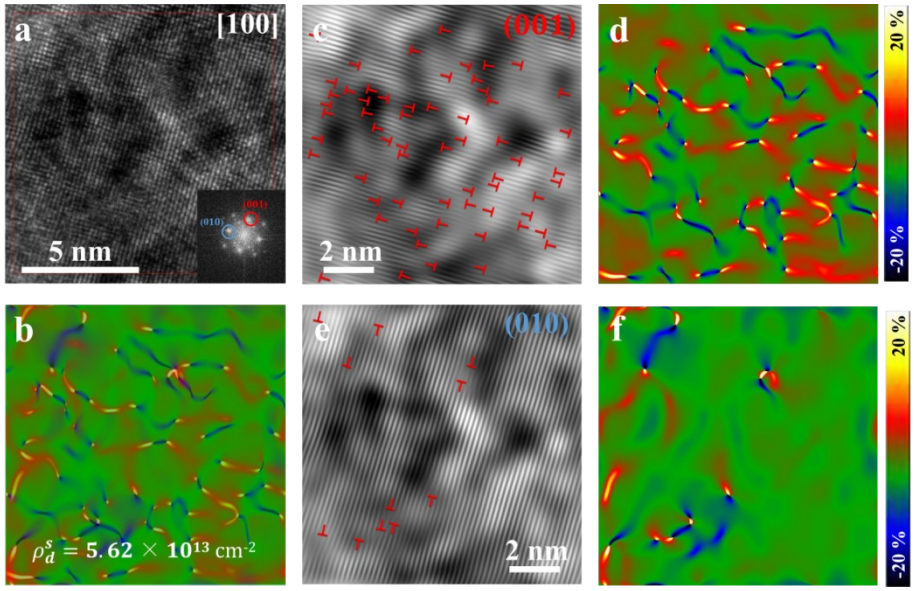

Supplementary Figure 4. a HR-TEM image of the D-$Ni_{3.5}Pd$ nanoparticles (removed from the D-$Ni_{3.5}Pd$/NF electrode by ultrasonication) along [100] zone axis and corresponding electron diffraction pattern by performing FFT on **a** ; **b** An overlay of strain components ε_{xx} and ε_{yy}, superimposed with the HR-TEM image, suggesting a high dislocation density of ρ_d^s = 5.62×10^{13} cm^{-2} on (100) plane. **c** IFFT image corresponding to diffraction spot 001, showing the (001) plane containing edge dislocations marked with symbol ⊥. **d** Contour plot of the strain component ε_{xx} by GPA analysis on (**c**). The color legend represents different strain, *i.e.*, green to dark blue relates to compressive strain and red to bright yellow corresponds to tensile strain. **e** IFFT image corresponding to diffraction spot 010, showing the (010) plane containing edge dislocations marked with symbol ⊥. **h** Contour plot of the strain component ε_{yy} by GPA analysis on (**e**).

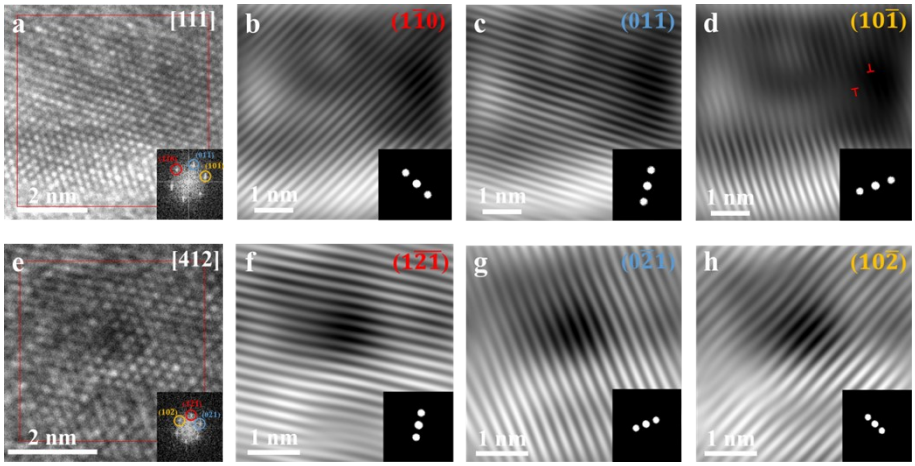

Supplementary Figure 5. a HR-TEM images and corresponding FFT image of the $Ni_{3.5}Pd$ nanoparticles along the crystal zone axis of [111]. **b-d** IFFT images corresponding to diffraction spots $1\bar{1}0$, $01\bar{1}$, and $10\bar{1}$, respectively, showing the $(1\bar{1}0)$, $(01\bar{1})$ and $(10\bar{1})$ planes containing almost no defects. **e** HR-TEM images and corresponding FFT image of the $Ni_{3.5}Pd$ nanoparticles along the crystal zone axis of [412]. **f-h** IFFT images corresponding to diffraction spots $12\bar{1}$, $02\bar{1}$, and $10\bar{2}$, respectively, showing the $(12\bar{1})$, $(02\bar{1})$ and $(10\bar{2})$ planes containing no defects.

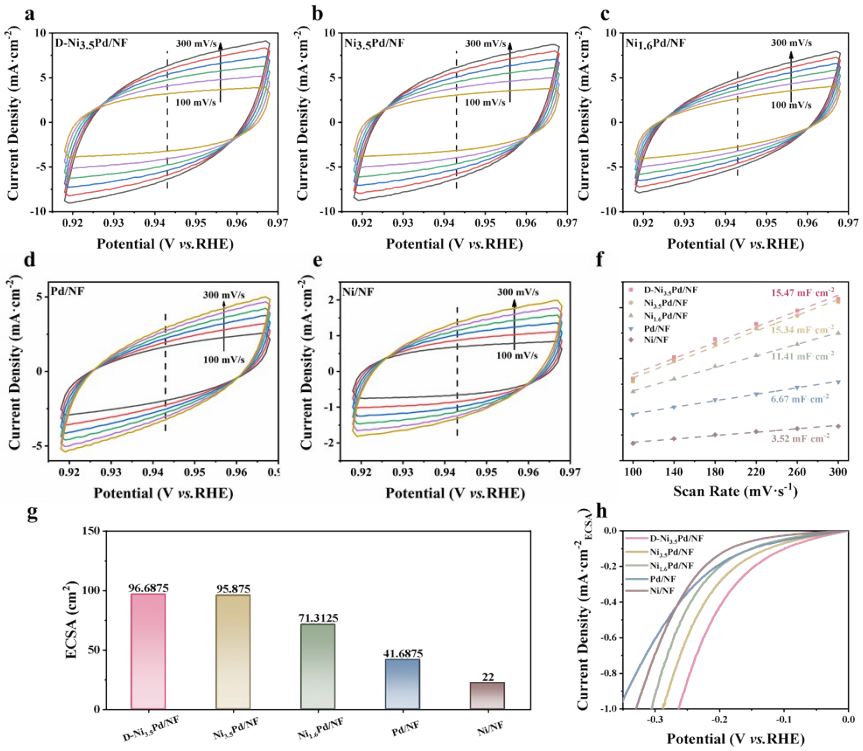

Supplementary Figure 6. Cyclic voltammograms at different scan rate in the region of -0.91 to -0.97 mV *vs.* Hg/HgO in 1 mol L^{-1} KOH for **a** D-$Ni_{3.5}Pd$/NF, **b** $Ni_{3.5}Pd$/NF, **c** $Ni_{1.6}Pd$/NF, **d** Pd/NF and **e** pure Ni foam electrodes. **f** Current density-scan rate curve for ECSA caculation. **g** ECSA of above electrodes. **h** Polarization curves after ECSA normalization of these electrodes.

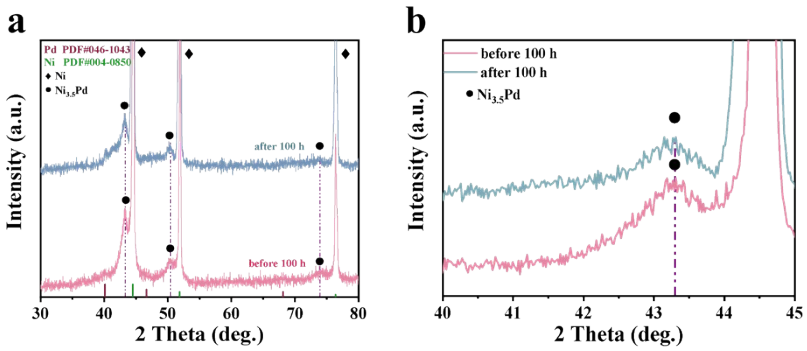

Supplementary Figure 7. a XRD patterns and **b** enlarged patterns in the range between 40° to 45°of the D-$Ni_{3.5}$Pd/NF electrode before or after electrochemical stability test.

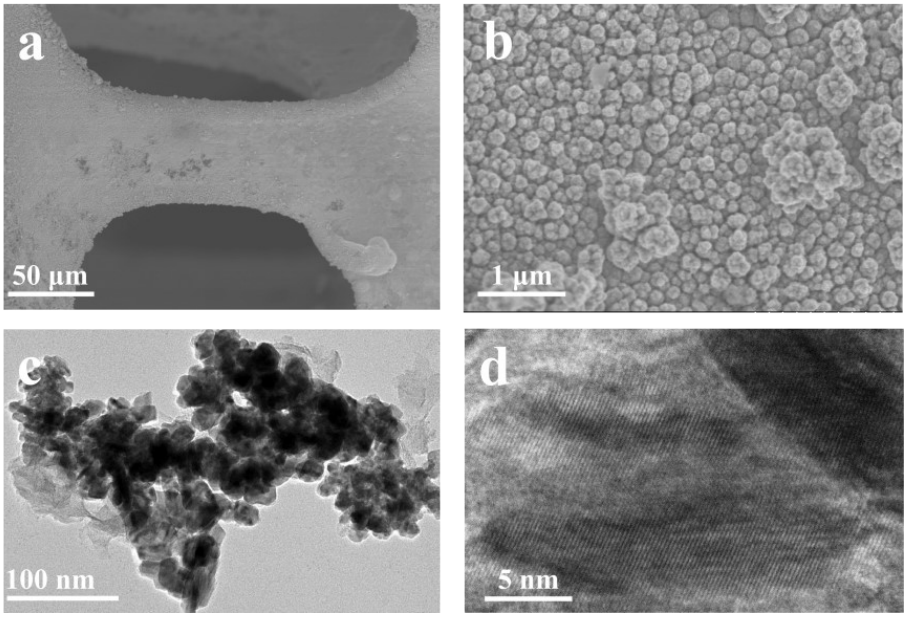

Supplementary Figure 8. a-b SEM images of the D-$Ni_{3.5}$Pd/NF electrode after long-term test. **c** TEM image of the D-$Ni_{3.5}$Pd nanaparticles removed from the D-$Ni_{3.5}$Pd/NF electrode after long-term test. **d** HR-TEM image of one D-$Ni_{3.5}$Pd nanaparticle after long-term test.

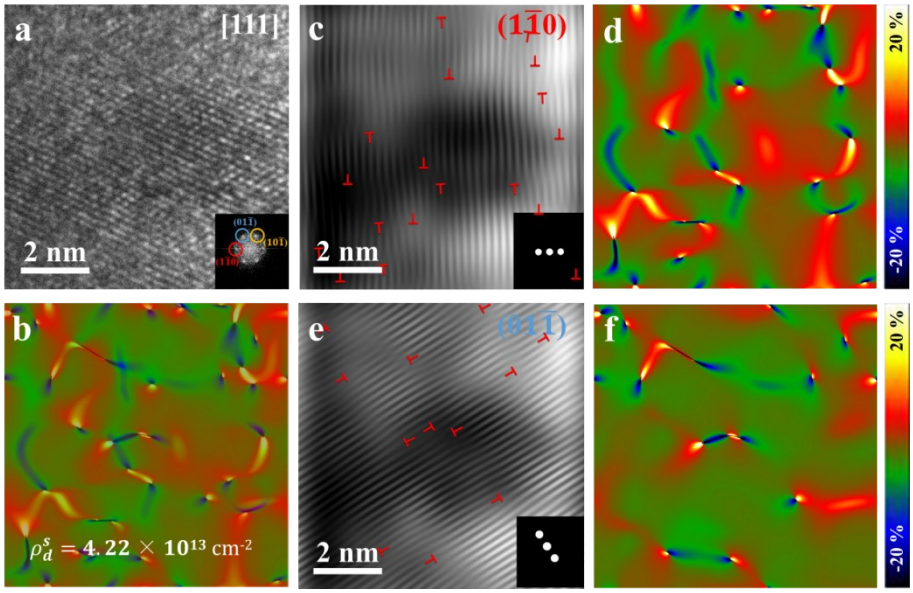

Supplementary Figure 9. a HR-TEM image of the D-$Ni_{3.5}Pd$ nanoparticles (removed from the D-$Ni_{3.5}Pd$/NF electrode after long-term test by ultrasonication) along [111] zone axis and corresponding electron diffraction pattern by performing FFT on (**a)** ; **b** An overlay of strain components ε_{xx} and ε_{yy}, superimposed with the HR-TEM image, suggesting a high dislocation density of ρ_d^s = 4.22×10^{13} cm^{-2} on (111) plane. **c** IFFT image corresponding to diffraction spot $1\bar{1}0$, showing the $(1\bar{1}0)$ plane containing edge dislocations marked with symbol ⊥. **d** Contour plot of the strain component ε_{xx} by GPA analysis on (**c**). The color legend represents different strain, *i.e.*, green to dark blue relates to compressive strain and red to bright yellow corresponds to tensile strain. **e** IFFT image corresponding to diffraction spot $01\bar{1}$, showing the $(01\bar{1})$ plane containing edge dislocations marked with symbol ⊥. **h** Contour plot of the strain component ε_{yy} by GPA analysis on (**e**).

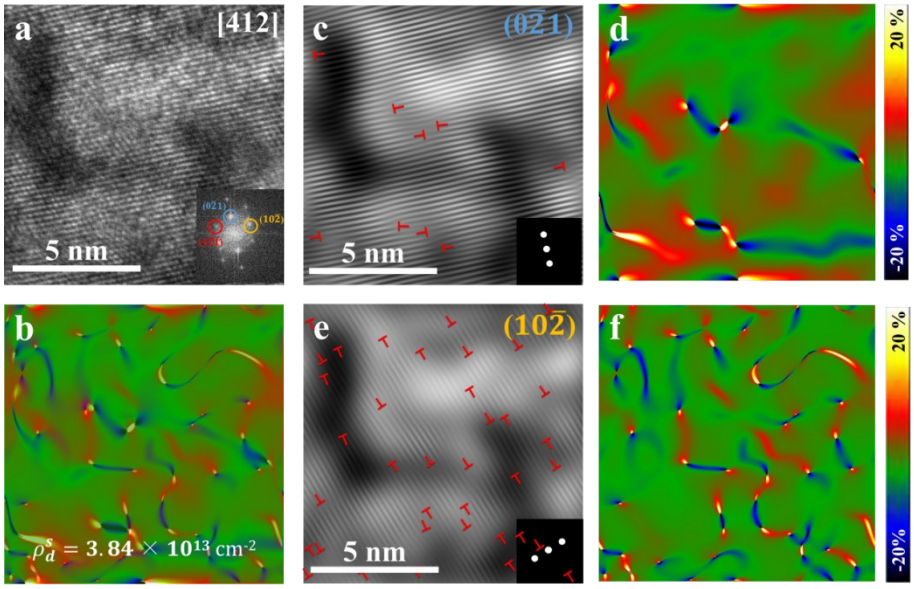

Supplementary Figure 10. a HR-TEM image of the D-$Ni_{3.5}$Pd nanoparticles (removed from the D-$Ni_{3.5}$Pd/NF electrode after long-term test by ultrasonication) along [412] zone axis and corresponding electron diffraction pattern by performing FFT on (**a)** ; **b** An overlay of strain components ε_{xx} and ε_{yy}, superimposed with the HR-TEM image, suggesting a high dislocation density of ρ_d^s = 3.84×10^{13} cm^{-2} on (412) plane. **c** IFFT image corresponding to diffraction spot $0\bar{2}1$, showing the ($0\bar{2}1$) plane containing edge dislocations marked with symbol ⊥. **d** Contour plot of the strain component ε_{xx} by GPA analysis on (**c**). The color legend represents different strain, *i.e.*, green to dark blue relates to compressive strain and red to bright yellow corresponds to tensile strain. **e** IFFT image corresponding to diffraction spot $10\bar{2}$, showing the ($10\bar{2}$) plane containing edge dislocations marked with symbol ⊥. **h** Contour plot of the strain component ε_{yy} by GPA analysis on (**e**).

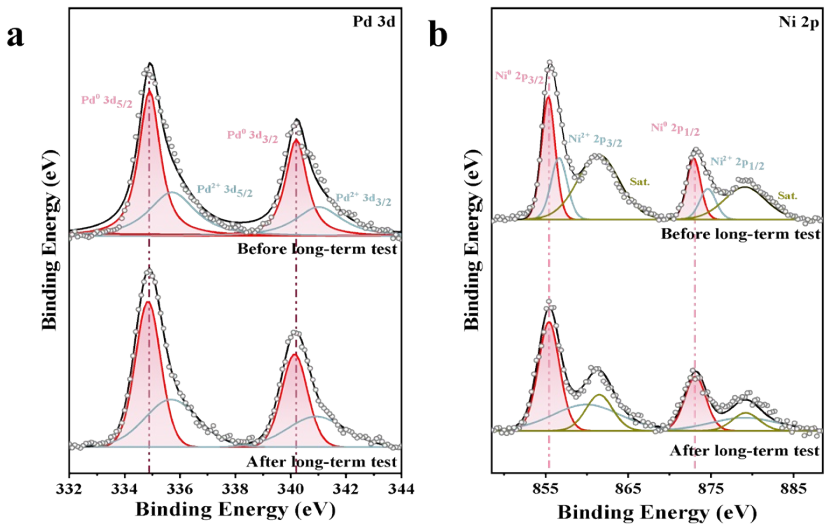

Supplementary Figure 11. High-resolution XPS spectra of **a** Pd 3d and **b** Ni 2p of D-$Ni_{3.5}$Pd/NF

electrode before or after long-term test.

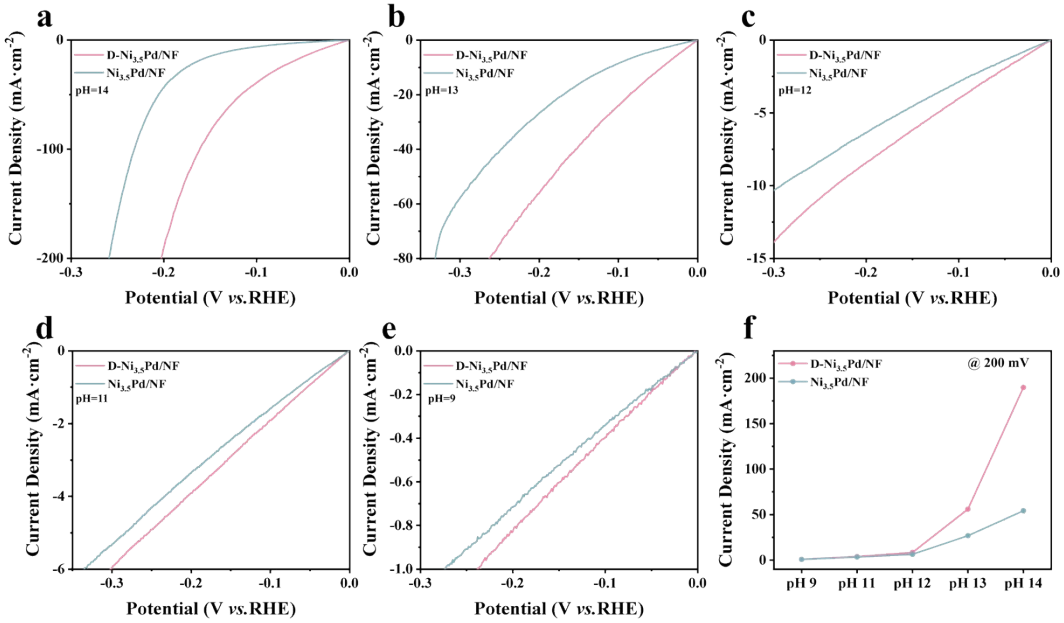

Supplementary Figure 12. a-e Polarization curves of D-$Ni_{3.5}$Pd/NF and $Ni_{3.5}$Pd/NF electrodes in alkine solution of various pH. **f** The pH-activity curve of D-$Ni_{3.5}$Pd/NF and $Ni_{3.5}$Pd/NF electrodes.

Supplementary Table 1. Compositions of electroplating solutions for electrodeposition.

	$NiCl_2 \cdot 6H_2O$	$PdCl_2$	H_3BO_3	NH_4Cl	$CH_3(CH_2)_{11}SO_4Na$	pH
$Ni_{1.6}Pd/NF$	10 mmol/L	5 mmol/L	40 mmol/L	25 mmol/L	160 mg/L	8
$Ni_{3.5}Pd/NF$	15 mmol/L	5 mmol/L	40 mmol/L	25 mmol/L	160 mg/L	8
Pd/NF	0	5 mmol/L	40 mmol/L	25 mmol/L	160 mg/L	8
Ni/NF	10 mmol/L	0	40 mmol/L	25 mmol/L	160 mg/L	8

Supplementary Table 2. TEM-EDS results of D-$Ni_{3.5}Pd$, $Ni_{3.5}Pd$ and $Ni_{1.6}Pd$ nanoparticles.

	Element	At(%)							Ratio
		Region 1	Region 2	Region 3	Region 4	Region 5	Region 6	Average	
D-$Ni_{3.5}Pd/NF$	Ni	78.76	78.51	78.25	77.50	77.30	77.04	77.89	3.5±0.2：
	Pd	21.24	21.49	21.75	22.50	22.70	22.96	22.11	1
$Ni_{3.5}Pd/NF$	Ni	78.35	77.97	77.83	77.30	77.12	77.01	77.59	3.5±0.3：
	Pd	21.65	22.03	22.17	22.70	22.88	22.99	22.41	1
$Ni_{1.6}Pd/NF$	Ni	62.81	61.91	60.90	61.77	61.54	61.42	62.13	1.6±0.1：
	Pd	37.19	38.09	39.10	38.23	38.46	38.58	37.87	1

Supplementary Table 3. Comparison of atomic percentages of Ni and Pd for D-$Ni_{3.5}Pd$, $Ni_{3.5}Pd$ and $Ni_{1.6}Pd$ nanoparticles determined by XPS measurements.

	Element	At(%)	Ratio
D-$Ni_{3.5}Pd/NF$	Ni	77.92	3.5:1
	Pd	22.08	
$Ni_{3.5}Pd/NF$	Ni	77.11	3.4:1
	Pd	22.89	
$Ni_{1.6}Pd/NF$	Ni	59.68	1.5:1
	Pd	40.32	

Supplementary Table 4. Dislocation densities on different crystal planes of D-$Ni_{3.5}Pd$ nanoparticles.

Crystal plane	Particle maximum cross-sectional area (nm^2)	Dislocation number	Dislocation density (cm^{-2})
(111)	**73.1**	**50**	**6.84×10^{13}**
(412)	**62.3**	**33**	**5.23×10^{13}**
(100)	**128.1**	**72**	**5.62×10^{13}**

Supplementary Table 5. Dislocation densities on different crystal planes of D-$Ni_{3.5}Pd$ nanoparticles after long-term test.

Crystal plane	Particle maximum cross-sectional area (nm^2)	Dislocation number	Dislocation density (nm^{-2})
(111)	**71.1**	**30**	**4.22×10^{13}**
(412)	**119.8**	**46**	**3.84×10^{13}**
(100)	**65.3**	**19**	**2.91×10^{13}**